光纤惯导角度随机游走误差传播特性研究

任 磊[1,2]，杜建邦[1,2]，邵春江[1,2]
（1. 北京航天自动控制研究所，北京 100854；2. 宇航智能控制技术国家级重点实验室，北京 100854）

摘 要：角度随机游走是光纤陀螺的一个重要技术指标，也是高精度光纤惯导系统的一项重要误差源。为了深入了解角度随机游走误差对系统精度的影响，从统计角度研究了该误差在导航过程中的传播特性。通过将角度随机游走对系统的影响等效为不相关的随机脉冲序列激励下的系统输出，推导了角度随机游走作用下导航误差的理论公式并进行了仿真验证。结果表明，所给出的理论表达式能够很好地描述角度随机游走误差的传播规律。通过解析表达式，可以在任意时间段对任何一只陀螺角度随机游走造成的系统误差进行定量分析，这对于系统性能评估、误差分析和设计工作都具有重要意义。

关键词：光纤陀螺；惯导系统；角度随机游走；误差传播特性；误差分析
中图分类号：V249.32^{+}2 **文献标识码**：A **文章编号**：1000-1328(2013)05-0617-08
DOI：10.3873/j.issn.1000-1328.2013.05.004

Study of Error Propagation Characteristics of FOG ARW in INS

REN Lei[1,2], DU Jian-bang[1,2], SHAO Chun-jiang[1,2]
(1. Beijing Aerospace Automatic Control Institute, Beijing 100854, China;
2. National Key Laboratory of Science and Technology on Aerospace Intelligent Control, Beijing 100854, China)

Abstract: Angle random walk (ARW) is a significant specification of FOG (Fiber Optic Gyro) and one of the critical error sources in INS (Inertial Navigation System). To recognize the effect of ARW on system accuracy thoroughly, propagation characteristics of navigation errors caused by ARW are investigated from the point of view of statistics. Analytical expressions for the standard deviation of navigation errors caused by ARW are developed by considering system errors owing to ARW as the output of the INS stimulated by incorrelate random pulse series. Computer simulation is made to validate the correctness of these expressions. The simulation result indicates that the theoretical expressions are used to describe propagation characteristics of navigation error caused by ARW well. The analytic expressions will help quantify to what extent ARW degrades the system accuracy over any time interval and for any one gyro. This is valuable to system performance evaluation, error analysis and design.

Key words: Fiber optic gyroscope; Inertial navigation systems; Angle random walk (ARW); Error propagation characteristics; Error analysis

0 引 言

光纤陀螺在精度、工艺、可靠性等方面所具有的优点使其在惯性导航领域获得了广泛应用，已成为惯性仪表的一个重要发展方向[1]。目前，国外光纤陀螺的研究和应用已达到很高的水平[2]。国内在光纤陀螺及其信号滤波、误差建模等方面的研究也取得了很大进展[3-5]，对高精度光纤惯导系统的需求也日益增强。对于系统级应用，与传统的机电陀螺相比，光纤陀螺有其特殊之处，因此对光纤陀螺中包含的与机电陀螺有较大差异的误差源及其在导航过程中的影响进行研究有助于高精度光纤惯导系统的设计和精度分析。

光纤陀螺与传统机电陀螺的一个重要区别就是

收稿日期：2012-09-25； 修回日期：2013-01-06

角速率输出中包含较大的白噪声,使得由于角速率白噪声积分后所产生的角度随机游走(以下简称为随机游走)误差成为光纤陀螺的主要技术指标之一,也成为高精度光纤惯导的一项重要误差源。理论上,采取其它系统级误差补偿技术后,随机游走误差成为唯一限制系统长期精度的因素[2]。从公开发表的文献看,国内对随机游走的研究主要集中在仪表级[6-9],从系统层面研究随机游走误差影响导航精度的比较少,且很大程度上是定性或从简化的导航误差方程入手进行分析[10-11]。文献[12-13]指出随机游走误差是限制罗经对准时间的关键因素,但没有对导航过程中随机游走引起的误差进行深入研究。文献[14]对此进行了分析,然而没有公开其研究成果,仅以东向位置误差为例作了简单说明。本文系统地研究了陀螺随机游走误差对导航精度的影响,从统计角度采用随机过程线性变换的冲激响应法推导了随机游走引起的位置、速度和姿态误差的理论表达式。本文虽然以光纤惯导为对象研究随机游走在导航过程中的表现,但结论适用于激光惯导及其它具有类似随机游走误差特征的惯导系统。

1 随机游走的概念及其统计特性

1.1 光纤陀螺随机游走误差

光纤陀螺中光电探测器、光纤环、光源等都会产生较大的角速率白噪声,积分后产生角度随机游走[8,15],体现为陀螺对角度的测量呈现出随机的"游走"特征。对系统级应用来说,陀螺误差项的产生机理并不重要,重要的是对系统性能的影响。因此,这里对于光纤陀螺随机游走的更深层次产生机理不做过多阐述,而着重从系统级应用角度分析随机游走误差对导航精度的影响。

1.2 随机游走误差的统计特性

根据1.1节,随机游走可以表示为

$$\theta(t) = \int_0^t w(\tau)\mathrm{d}\tau \tag{1}$$

式中,$w(\tau)$ 为角速率白噪声,$\theta(t)$ 为积分后的角度随机游走。

由式(1),可以得到随机游走的统计量:

(1) 均值

$$\mu(t) = \mathrm{E}\{\theta(t)\} = \int_0^t \mathrm{E}\{w(\tau)\}\mathrm{d}\tau = 0 \tag{2}$$

(2) 标准差

$\theta(t)$ 的方差为

$$\begin{aligned}\sigma^2(t) &= \mathrm{E}\{\theta^2(t)\} = \mathrm{E}\left\{\int_0^t w(\tau_1)\mathrm{d}\tau_1 \int_0^t w(\tau_2)\mathrm{d}\tau_2\right\}\\ &= \mathrm{E}\left\{\int_0^t\int_0^t w(\tau_1)w(\tau_2)\mathrm{d}\tau_1\mathrm{d}\tau_2\right\}\\ &= \int_0^t\int_0^t \mathrm{E}\{w(\tau_1)w(\tau_2)\}\mathrm{d}\tau_1\mathrm{d}\tau_2\end{aligned} \tag{3}$$

$w(\tau)$ 为白噪声,存在如下关系

$$\mathrm{E}\{w(\tau_1)w(\tau_2)\} = \begin{cases}0, & \tau_1 \neq \tau_2\\ K^2, & \tau_1 = \tau_2\end{cases} \tag{4}$$

式中,K^2 为 $w(\tau)$ 的方差。将式(4)代入式(3),并令 $\tau_1 = \tau_2 = \tau$ 得到

$$\sigma^2(t) = \int_0^t K^2\mathrm{d}\tau = K^2 t \tag{5}$$

则标准差

$$\sigma(t) = K\sqrt{t} \tag{6}$$

式中 K 即为随机游走系数。从式(2)、(6)可知,随机游走是均值为零,标准差随时间平方根增长的随机过程,而随机游走系数 K 表征了增长的强度。

2 随机游走引起的导航误差解析表达式

2.1 系统误差方程

惯导系统误差模型可由下列3个基本方程表示[16]:

$$\begin{aligned}\dot{\boldsymbol{\psi}} &= -[\boldsymbol{\omega}_{in}^n\times]\boldsymbol{\psi} + \delta\boldsymbol{\omega}_{in}^n - \boldsymbol{C}_b^n\delta\boldsymbol{\omega}_{ib}^b\\ \delta\dot{\boldsymbol{v}} &= [\boldsymbol{f}^n\times]\boldsymbol{\psi} + \boldsymbol{C}_b^n\delta\boldsymbol{f}^b - [(2\boldsymbol{\omega}_{ie}^n + \boldsymbol{\omega}_{en}^n)\times]\delta\boldsymbol{v} -\\ &\quad [(2\delta\boldsymbol{\omega}_{ie}^n + \delta\boldsymbol{\omega}_{en}^n)\times]\boldsymbol{v} - \delta\boldsymbol{g}\\ \delta\dot{\boldsymbol{p}} &= \delta\boldsymbol{v}\end{aligned} \tag{7}$$

式中,$[\boldsymbol{\Lambda}\times]$ 表示向量 $\boldsymbol{\Lambda}$ 对应的反对称矩阵。

不考虑高度通道及重力变化,导航坐标系取当地东、北、天地理坐标系(E、N、U),由式(7)展开可得到系统误差方程:

$$\dot{\boldsymbol{X}} = \boldsymbol{A}\boldsymbol{X} + \boldsymbol{G}\boldsymbol{W} \tag{8}$$

式中,$\boldsymbol{X} = [\psi_E \quad \psi_N \quad \psi_U \quad \delta v_E \quad \delta v_N \quad \delta L \quad \delta\lambda]^{\mathrm{T}}$ 表示系统导航参数误差,其中,$\boldsymbol{\psi}$,$\delta\boldsymbol{v}$,$\delta\boldsymbol{p}$ 为姿态、速度和位置误差向量,δL、$\delta\lambda$ 分别为纬度和经度误差;$\boldsymbol{W} = [\delta w_x, \delta w_y, \delta w_z, \delta f_x, \delta f_y, \delta f_z]^{\mathrm{T}}$ 表示陀螺和加表误差;

$$\boldsymbol{A} = \begin{bmatrix}\boldsymbol{A}_1 & \boldsymbol{A}_2\\ \boldsymbol{A}_3 & \boldsymbol{A}_4\end{bmatrix}, \boldsymbol{G} = \begin{bmatrix}\boldsymbol{G}_1 & \boldsymbol{0}_{3\times3}\\ \boldsymbol{0}_{2\times3} & \boldsymbol{G}_2\\ \boldsymbol{0}_{2\times3} & \boldsymbol{0}_{2\times3}\end{bmatrix}$$

$$\boldsymbol{A}_1 = \begin{bmatrix} 0 & \omega_E \sin L & -\omega_E \cos L \\ -\omega_E \sin L & 0 & 0 \\ \omega_E \cos L & 0 & 0 \end{bmatrix}$$

$$\boldsymbol{A}_2 = \begin{bmatrix} 0 & -\dfrac{1}{R} & 0 & 0 \\ \dfrac{1}{R} & 0 & -\omega_E \sin L & 0 \\ \dfrac{\tan L}{R} & 0 & \omega_E \cos L & 0 \end{bmatrix}$$

$$\boldsymbol{A}_3 = \begin{bmatrix} 0 & -g & 0 \\ g & 0 & 0 \\ 0 & 0 & 0 \\ 0 & 0 & 0 \end{bmatrix}$$

$$\boldsymbol{A}_4 = \begin{bmatrix} 0 & 2\omega_E \sin L & 0 & 0 \\ -2\omega_E \sin L & 0 & 0 & 0 \\ 0 & \dfrac{1}{R} & 0 & 0 \\ \dfrac{1}{R \cos L} & 0 & 0 & 0 \end{bmatrix}$$

$$\boldsymbol{G}_1 = \begin{bmatrix} -C_{11} & -C_{12} & -C_{13} \\ -C_{21} & -C_{22} & -C_{23} \\ -C_{31} & -C_{32} & -C_{33} \end{bmatrix}$$

$$\boldsymbol{G}_2 = \begin{bmatrix} C_{11} & C_{12} & C_{13} \\ C_{21} & C_{22} & C_{23} \end{bmatrix}$$

上述系数矩阵中 ω_E 为地球自转角速度,R 为地球半径,L 为当地地理纬度,g 为重力加速度;$C_{ij}(i, j = 1, 2, 3)$ 为姿态矩阵元素。

2.2　随机游走引起的导航误差理论推导

根据随机游走的产生机理,随机游走对导航精度的影响可以看成是不相关的随机脉冲序列作用于导航系统。任一时刻的导航误差则是之前所有随机脉冲输入在该时刻产生的误差效应的卷积[17],可描述为

$$y(t) = \int_0^t f(t-\tau) w(\tau) \mathrm{d}\tau \tag{9}$$

式中,$y(t)$ 表示导航参数误差,$w(\tau)$ 为导航坐标系中角速率状态的白噪声,$f(t)$ 为系统响应脉冲输入的权函数。由式(9),导航误差的自相关函数可以表示为:

$$\phi(t_1, t_2) = \mathrm{E}\left\{\int_0^{t_1} f(t_1-\tau_1) w(\tau_1) \mathrm{d}\tau_1 \cdot \int_0^{t_2} f(t_2-\tau_2) w(\tau_2) \mathrm{d}\tau_2\right\}$$

$$= \mathrm{E}\left\{\int_0^{t_1}\int_0^{t_2} f(t_1-\tau_1) f(t_2-\tau_2) w(\tau_1) w(\tau_2) \mathrm{d}\tau_1 \mathrm{d}\tau_2\right\} \tag{10}$$

根据式(9),$y(t)$ 可以认为是 $w(\tau)$ 经导航系统线性变换后的随机输出过程。在求取输出过程的自相关函数时计算数学期望与系统权函数无关[18-19]。因此,式(10)可写为

$$\phi(t_1, t_2) = \int_0^{t_1}\int_0^{t_2} f(t_1-\tau_1) f(t_2-\tau_2) \cdot \mathrm{E}\{w(\tau_1) w(\tau_2)\} \mathrm{d}\tau_1 \mathrm{d}\tau_2 \tag{11}$$

将式(4)代入式(11),并进行相应的积分运算可得:

$$\phi(t, t) = K^2 \int_0^t f^2(\tau) \mathrm{d}\tau \tag{12}$$

对式(9)两边求取数学期望,根据式(2)易知 $y(t)$ 的均值为零,而对于均值为零的随机过程,相关时间为零时的自相关函数就表示随机过程在 t 时刻的方差,因此,式(12)即为导航误差的方差,相应的导航误差的标准差可以表示为:

$$\sigma(t) = K\left[\int_0^t f^2(\tau) \mathrm{d}\tau\right]^{1/2} \tag{13}$$

由导航误差方程(8),系统状态转移矩阵 $\boldsymbol{\Phi}(t) = \mathrm{e}^{\boldsymbol{A}t}$。权函数 $f(t)$ 即是 $\boldsymbol{\Phi}(t)$ 的元素,因此,根据误差方程(8)计算矩阵指数 $\mathrm{e}^{\boldsymbol{A}t}$ 得到权函数 $f(t)$,代入式(13)就可以得到随机游走激励下的导航误差标准差。限于篇幅,这里仅给出脉冲响应权函数及导航误差标准差的部分推导结果:

$$f_{EN}^P(t) = R(-\cos^2 L - \sin^2 L \cos\omega_E t + \cos\omega_S t \cos\omega_F t)$$

$$f_{NE}^P(t) = R(\cos\omega_E t - \cos\omega_S t \cos\omega_F t)$$

$$f_{NU}^P(t) = R\cos L\left(-\sin w_E t + \frac{\omega_E}{\omega_S}\sin\omega_S t \cos\omega_F t\right)$$

$$f_{EU}^P(t) = R\cos L\left(\sin L \cos\omega_E t + \frac{\omega_E}{\omega_S}\sin\omega_S t \sin\omega_F t - \sin L\right)$$

$$f_{EN}^V(t) = R(\omega_E \sin^2 L \sin\omega_E t - \omega_S \sin\omega_S t \cos\omega_F t - \omega_F \cos\omega_S t \sin\omega_F t)$$

$$f_{NE}^V(t) = R(-\omega_E \sin\omega_E t + \omega_S \sin\omega_S t \cos\omega_F t + \omega_F \cos\omega_S t \sin\omega_F t)$$

$$f_{EU}^V(t) = R\omega_E \cos L(-\sin L \sin\omega_E t + \cos\omega_S t \sin\omega_F t)$$

$$f_{NU}^V(t) = R\omega_E \cos L(-\cos\omega_E t + \cos\omega_S t \cos\omega_F t)$$

$$f_{UE}^{\psi}(t) = \sec L \sin\omega_E t - \tan L \cos\omega_S t \sin\omega_F t$$

$$f_{UN}^{\psi}(t) = \tan L(-\cos\omega_E t + \cos\omega_S t\cos\omega_F t)$$

$$f_{UU}^{\psi}(t) = \cos\omega_E t + \frac{\omega_F}{\omega_S}\sin\omega_S t\sin\omega_F t + \frac{\omega_F^2}{\omega_S^2}\cos\omega_S t\cos\omega_F t \tag{14}$$

式中，ω_S 为舒拉振荡角频率，ω_F 为付科振荡角频率；权函数 $f_{XY}^{Z}(t)$ 上标 $Z = P、V、\psi$ 表示位置、速度、姿态，下标 XY 表示 X 向导航参数误差对 Y 向输入的响应，其中 $X = E、N、U$，$Y = E、N、U$。上式代入式(13)，得到随机游走激励下的导航误差：

$$\sigma_{EN}^{P}(t) = RK_N\left\{\left(\cos^4 L + \frac{1}{2}\sin^4 L + \frac{1}{4}\right)t + \frac{\sin^2 2L}{2\omega_E}\sin\omega_E t + \frac{1}{4}\left(\frac{\sin^4 L}{\omega_E}\sin 2\omega_E t + \frac{\sin 2\omega_S t}{2\omega_S} + \frac{\sin 2\omega_F t}{2\omega_F}\right) - \cos^2 L\left[\frac{\sin(\omega_S+\omega_F)t}{\omega_S+\omega_F} + \frac{\sin(\omega_S-\omega_F)t}{\omega_S-\omega_F}\right] + \frac{1}{16}\left[\frac{\sin 2(\omega_S+\omega_F)t}{\omega_S+\omega_F} + \frac{\sin 2(\omega_S-\omega_F)t}{\omega_S-\omega_F}\right] - \frac{\sin^2 L}{2}\left[\frac{\sin(\omega_S+\omega_E+\omega_F)t}{\omega_S+\omega_E+\omega_F} + \frac{\sin(\omega_S+\omega_E-\omega_F)t}{\omega_S+\omega_E-\omega_F} + \frac{\sin(\omega_S-\omega_E+\omega_F)t}{\omega_S-\omega_E+\omega_F} + \frac{\sin(\omega_S-\omega_E-\omega_F)t}{\omega_S-\omega_E-\omega_F}\right]\right\}^{\frac{1}{2}}$$

$$\sigma_{NE}^{P}(t) = RK_E\left\{\frac{3}{4}t + \frac{1}{8}\left(\frac{\sin 2\omega_S t}{\omega_S} + \frac{2\sin 2\omega_E t}{\omega_E} + \frac{\sin 2\omega_F t}{\omega_F}\right) + \frac{1}{16}\left[\frac{\sin 2(\omega_S+\omega_F)t}{\omega_S+\omega_F} + \frac{\sin 2(\omega_S-\omega_F)t}{\omega_S-\omega_F}\right] - \frac{1}{2}\left[\frac{\sin(\omega_S+\omega_E+\omega_F)t}{\omega_S+\omega_E+\omega_F} + \frac{\sin(\omega_S-\omega_E-\omega_F)t}{\omega_S-\omega_E-\omega_F} + \frac{\sin(\omega_S+\omega_E-\omega_F)t}{\omega_S+\omega_E-\omega_F} + \frac{\sin(\omega_S-\omega_E+\omega_F)t}{\omega_S-\omega_E+\omega_F}\right]\right\}^{\frac{1}{2}}$$

$$\sigma_{NU}^{P}(t) = RK_U\cos L\left\{\left(\frac{1}{2} + \frac{\omega_E^2}{4\omega_S^2}\right)t - \frac{1}{8}\left(\frac{\omega_E^2}{\omega_S^3}\sin 2\omega_S t + \frac{2}{\omega_E}\sin 2\omega_E t - \frac{\omega_E^2}{\omega_S^2\omega_F}\sin 2\omega_F t\right) - \frac{\omega_E^2}{16\omega_S^2}\left[\frac{\sin 2(\omega_S+\omega_F)t}{\omega_S+\omega_F} + \frac{\sin 2(\omega_S-\omega_F)t}{\omega_S-\omega_F}\right] + \frac{\omega_F}{2\omega_S}\left[\frac{\sin(\omega_S+\omega_E+\omega_F)t}{\omega_S+\omega_E+\omega_F} + \frac{\sin(\omega_S+\omega_E-\omega_F)t}{\omega_S+\omega_E-\omega_F} - \frac{\sin(\omega_S-\omega_E+\omega_F)t}{\omega_S-\omega_E+\omega_F} - \frac{\sin(\omega_S-\omega_E-\omega_F)t}{\omega_S-\omega_E-\omega_F}\right]\right\}^{\frac{1}{2}}$$

$$\sigma_{EU}^{P}(t) = RK_U\cos L\left\{\left(\frac{3}{2}\sin^2 L + \frac{\omega_E^2}{4\omega_S^2}\right)t - \frac{2\sin^2 L}{\omega_E}\sin\omega_E t - \frac{1}{8}\left(\frac{\omega_E^2}{\omega_S^3}\sin 2\omega_S t - \frac{2\sin^2 L}{\omega_E}\sin 2\omega_E t + \frac{\omega_E^2}{\omega_S^2\omega_F}\sin 2\omega_F t\right) + \frac{\omega_F}{\omega_S}\left[\frac{\sin(\omega_S+\omega_F)t}{\omega_S+\omega_F} - \frac{\sin(\omega_S-\omega_F)t}{\omega_S-\omega_F}\right] + \frac{\omega_E^2}{16\omega_S^2}\left[\frac{\sin 2(\omega_S+\omega_F)t}{\omega_S+\omega_F} + \frac{\sin 2(\omega_S-\omega_F)t}{\omega_S-\omega_F}\right] - \frac{w_F}{2w_S}\left[\frac{\sin(\omega_S+\omega_E+\omega_F)t}{\omega_S+\omega_E+\omega_F} + \frac{\sin(\omega_S-\omega_E+\omega_F)t}{\omega_S-\omega_E+\omega_F} - \frac{\sin(\omega_S+\omega_E-\omega_F)t}{\omega_S+\omega_E-\omega_F} - \frac{\sin(\omega_S-\omega_E-\omega_F)t}{\omega_S-\omega_E-\omega_F}\right]\right\}^{\frac{1}{2}}$$

$$\sigma_{EN}^{V}(t) = RK_N\left\{\frac{1}{4}(\omega_S^2 + 2\omega_E^2\sin^4 L + \omega_F^2)t - \frac{1}{8}\left(\frac{\omega_S^2-\omega_F^2}{\omega_S}\sin 2\omega_S t + \frac{2\omega_E^2\sin^4 L}{\omega_E}\sin 2\omega_E t - \frac{\omega_S^2-\omega_F^2}{\omega_F}\sin 2\omega_F t\right) - \frac{1}{16}(w_S^2 + w_F^2)\left[\frac{\sin 2(w_S+w_F)t}{w_S+w_F} + \frac{\sin 2(w_S-w_F)t}{w_S-w_F}\right] - \frac{1}{8}\omega_S\omega_F\left[\frac{\sin 2(\omega_S+\omega_F)t}{\omega_S+\omega_F} - \frac{\sin 2(\omega_S-\omega_F)t}{\omega_S-\omega_F}\right] + \frac{\omega_E(\omega_S+\omega_F)\sin^2 L}{2}\left[\frac{\sin(\omega_S+\omega_E+\omega_F)t}{\omega_S+\omega_E+\omega_F} - \frac{\sin(\omega_S-\omega_E+\omega_F)t}{\omega_S-\omega_E+\omega_F}\right] + \frac{\omega_E(\omega_S-\omega_F)\sin^2 L}{2}\left[\frac{\sin(\omega_S+\omega_E-\omega_F)t}{\omega_S+\omega_E-\omega_F} - \frac{\sin(\omega_S-\omega_E-\omega_F)t}{\omega_S-\omega_E-\omega_F}\right]\right\}^{\frac{1}{2}}$$

$$\sigma_{NE}^{V}(t) = RK_E\left\{\frac{1}{4}(\omega_S^2 + 2\omega_E^2 + \omega_F^2)t - \frac{1}{8}\left(\frac{\omega_S^2-\omega_F^2}{\omega_S}\sin 2\omega_S t + \frac{2\omega_E^2}{\omega_E}\sin 2\omega_E t - \frac{\omega_S^2-\omega_F^2}{\omega_F}\sin 2\omega_F t\right) -$$

$$\frac{\omega_S^2+\omega_F^2}{16}\left[\frac{\sin2(\omega_S+\omega_F)t}{\omega_S+\omega_F}+\frac{\sin2(\omega_S-\omega_F)t}{\omega_S-\omega_F}\right]-\frac{1}{8}\omega_S\omega_F\left[\frac{\sin2(\omega_S+\omega_F)t}{\omega_S+\omega_F}-\frac{\sin2(\omega_S-\omega_F)t}{\omega_S-\omega_F}\right]+$$

$$\frac{\omega_E(\omega_S+\omega_F)}{2}\left[\frac{\sin(\omega_S+\omega_E+\omega_F)t}{\omega_S+\omega_E+\omega_F}-\frac{\sin(\omega_S-\omega_E+\omega_F)t}{\omega_S-\omega_E+\omega_F}\right]+$$

$$\left.\frac{\omega_E(\omega_S-\omega_F)}{2}\left[\frac{\sin(\omega_S+\omega_E-\omega_F)t}{\omega_S+\omega_E-\omega_F}-\frac{\sin(\omega_S-\omega_E-\omega_F)t}{\omega_S-\omega_E-\omega_F}\right]\right\}^{\frac{1}{2}}$$

$$\sigma_{EU}^{V}(t)=RK_U\omega_E\cos L\left\{\left(\frac{1}{2}\sin^2L+\frac{1}{4}\right)t+\frac{1}{8}\left(\frac{\sin2\omega_St}{\omega_S}-\frac{2\sin^2L}{\omega_E}\sin2\omega_Et-\frac{\sin2\omega_Ft}{\omega_F}\right)-\right.$$

$$\frac{1}{16}\left[\frac{\sin2(\omega_S+\omega_F)t}{\omega_S+\omega_F}+\frac{\sin2(\omega_S-\omega_F)t}{\omega_S-\omega_F}\right]+\frac{\sin L}{2}\left[\frac{\sin(\omega_S+\omega_E+\omega_F)t}{\omega_S+\omega_E+\omega_F}+\frac{\sin(\omega_S-\omega_E-\omega_F)t}{\omega_S-\omega_E-\omega_F}-\right.$$

$$\left.\left.\frac{\sin(\omega_S+\omega_E-\omega_F)t}{\omega_S+\omega_E-\omega_F}-\frac{\sin(\omega_S-\omega_E+\omega_F)t}{\omega_S-\omega_E+\omega_F}\right]\right\}^{\frac{1}{2}}$$

$$\sigma_{NU}^{V}(t)=RK_U\omega_E\cos L\left\{\frac{3}{4}t+\frac{1}{8}\left(\frac{\sin2\omega_St}{\omega_S}+\frac{2\sin2\omega_Et}{\omega_E}+\frac{\sin2\omega_Ft}{\omega_F}\right)+\frac{1}{16}\left[\frac{\sin2(\omega_S+\omega_F)t}{\omega_S+\omega_F}+\frac{\sin2(\omega_S-\omega_F)t}{\omega_S-\omega_F}\right]-\right.$$

$$\left.\frac{1}{2}\left[\frac{\sin(\omega_S+\omega_E+\omega_F)t}{\omega_S+\omega_E+\omega_F}+\frac{\sin(\omega_S-\omega_E-\omega_F)t}{\omega_S-\omega_E-\omega_F}+\frac{\sin(\omega_S+\omega_E-\omega_F)t}{\omega_S+\omega_E-\omega_F}+\frac{\sin(\omega_S-\omega_E+\omega_F)t}{\omega_S-\omega_E+\omega_F}\right]\right\}^{\frac{1}{2}}$$

$$\sigma_{UE}^{\psi}(t)=K_E\left\{\left(\frac{3}{4}\tan^2L+\frac{1}{2}\right)t+\frac{1}{8}\left(\frac{\tan^2L}{\omega_S}\sin2\omega_St-\frac{2\sec^2L}{\omega_E}\sin2\omega_Et-\frac{\tan^2L}{\omega_F}\sin2\omega_Ft\right)-\right.$$

$$\frac{\tan^2L}{16}\left[\frac{\sin2(\omega_S+\omega_F)t}{\omega_S+\omega_F}+\frac{\sin2(\omega_S-\omega_F)t}{\omega_S-\omega_F}\right]+\sec L\tan L\left[\frac{\sin(\omega_S+\omega_E+\omega_F)t}{\omega_S+\omega_E+\omega_F}+\frac{\sin(\omega_S-\omega_E-\omega_F)t}{\omega_S-\omega_E-\omega_F}-\right.$$

$$\left.\left.\frac{\sin(\omega_S+\omega_E-\omega_F)t}{\omega_S+\omega_E-\omega_F}-\frac{\sin(\omega_S-\omega_E+\omega_F)t}{\omega_S-\omega_E+\omega_F}\right]\right\}^{\frac{1}{2}}$$

$$\sigma_{UN}^{\psi}(t)=K_N\tan L\left\{\frac{3}{4}t+\frac{1}{8}\left(\frac{\sin2\omega_St}{\omega_S}+\frac{2\sin2\omega_Et}{\omega_E}+\frac{\sin2\omega_Ft}{\omega_F}\right)+\frac{1}{16}\left[\frac{\sin2(\omega_S+\omega_F)t}{\omega_S+\omega_F}+\frac{\sin2(\omega_S-\omega_F)t}{\omega_S-\omega_F}\right]-\right.$$

$$\left.\frac{1}{2}\left[\frac{\sin(\omega_S+\omega_E+\omega_F)t}{\omega_S+\omega_E+\omega_F}+\frac{\sin(\omega_S+\omega_E-\omega_F)t}{\omega_S+\omega_E-\omega_F}+\frac{\sin(\omega_S-\omega_E+\omega_F)t}{\omega_S-\omega_E+\omega_F}+\frac{\sin(\omega_S-\omega_E-\omega_F)t}{\omega_S-\omega_E-\omega_F}\right]\right\}^{\frac{1}{2}}$$

$$\sigma_{UU}^{\psi}(t)=K_U\left\{\left(\frac{1}{2}+\frac{\omega_F^2}{4\omega_S^2}+\frac{\omega_F^4}{4\omega_S^4}\right)t+\frac{1}{8}\left[\left(\frac{\omega_F^4}{\omega_S^4}-\frac{\omega_F^2}{\omega_S^2}\right)\frac{\sin2\omega_St}{\omega_S}+\frac{2\sin2\omega_Et}{\omega_E}+\left(\frac{\omega_F^4}{\omega_S^4}-\frac{\omega_F^2}{\omega_S^2}\right)\frac{\sin2\omega_Ft}{\omega_F}\right]-\right.$$

$$\frac{\omega_F^3}{8\omega_S^3}\left[\frac{\sin2(\omega_S+\omega_F)t}{\omega_S+\omega_F}-\frac{\sin2(\omega_S-\omega_F)t}{\omega_S-\omega_F}\right]+\frac{1}{16}\left(\frac{\omega_F^4}{\omega_S^4}+\frac{\omega_F^2}{\omega_S^2}\right)\left[\frac{\sin2(\omega_S+\omega_F)t}{\omega_S+\omega_F}+\frac{\sin2(\omega_S-\omega_F)t}{\omega_S-\omega_F}\right]-$$

$$\frac{1}{2}\left(\frac{\omega_F}{\omega_S}-\frac{\omega_F^2}{\omega_S^2}\right)\left[\frac{\sin(\omega_S+\omega_E+\omega_F)t}{\omega_S+\omega_E+\omega_F}+\frac{\sin(\omega_S-\omega_E+\omega_F)t}{\omega_S-\omega_E+\omega_F}\right]+$$

$$\left.\frac{1}{2}\left(\frac{\omega_F}{\omega_S}+\frac{\omega_F^2}{\omega_S^2}\right)\left[\frac{\sin(\omega_S+\omega_E-\omega_F)t}{\omega_S+\omega_E-\omega_F}+\frac{\sin(\omega_S-\omega_E-\omega_F)t}{\omega_S-\omega_E-\omega_F}\right]\right\}^{\frac{1}{2}}\tag{15}$$

式中，K_E、K_N 和 K_U 分别表示等效的东向、北向和天向随机游走系数，上下标的定义和式(14) 相同，关于等效随机游走将在下一节中说明。

3　仿真验证

3.1　仿真条件与方法

为了对导出的理论公式进行验证，利用实际的

导航解算算法和100组0.003(°)/$\sqrt{\text{h}}$的随机游走样本序列,计算系统在随机游走序列激励下的导航误差,对得到的100组结果求取各导航参数的标准差,并与由式(15)得到的理论值进行比较。其中,纬度L = 39.9121°(北纬);重力加速度g = 9.8m/s^2;地球半径R = 6378137m。

随机游走引起的导航误差的理论表达式(15)反映的是系统受等效的东向、北向和天向随机游走的影响。由误差方程(8),导航坐标系中的等效随机游走可以表示为

$$(w_E \quad w_N \quad w_U)^{\mathrm{T}} = -\boldsymbol{C}_b^n(t)(\delta w_x \quad \delta w_y \quad \delta w_z)^{\mathrm{T}} \tag{16}$$

式中$\boldsymbol{C}_b^n(t) = (C_{ij})_{i,j=1,2,3}$为姿态矩阵;$w_E$、$w_N$、$w_U$分别为等效的东向、北向和天向陀螺随机游走误差。在导航过程中$\boldsymbol{C}_b^n(t)$不断变化,若加在陀螺数据上的随机游走量值不变,那么由式(16)可知,等效的东向、北向和天向随机游走量值将随姿态矩阵$\boldsymbol{C}_b^n(t)$而变化。由于不同方向上的随机游走对系统的影响程度不同,这样就不能通过仿真结果验证式(15)的正确性,因此,为了保证仿真过程中始终只有一个方向(E、N、U)的随机游走参与导航解算,应作如下处理:

$$(\delta w_x \quad \delta w_y \quad \delta w_z)^{\mathrm{T}} = \boldsymbol{C}_n^b(t)(w_E \quad w_N \quad w_U)^{\mathrm{T}} \tag{17}$$

δw_x、δw_y、δw_z是仿真时需要分别加在x、y、z轴陀螺数据上的随机游走误差。

3.2 仿真结果

图1、图2和图3分别以东向位置、北向速度和航向为例对随机游走引起的位置、速度和姿态误差的理论值和仿真结果进行了比较。从图中可以直观地看出,由理论公式得到的导航误差和仿真结果能够很好地吻合,这就验证了理论公式的正确性。

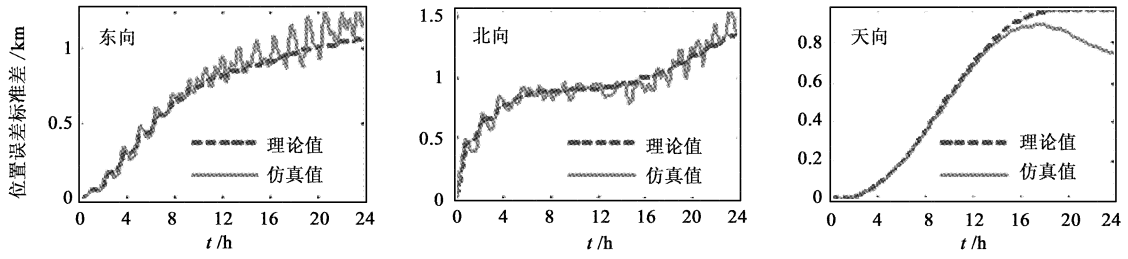

图1 等效东向/北向/天向随机游走引起的东向位置误差标准差理论和仿真比较

Fig. 1 Comparison of theory and simulation standard deviation of east position error due to equivalent east/north/up ARW

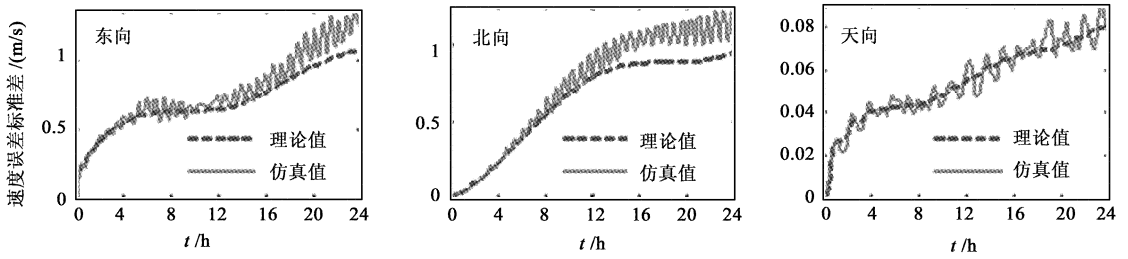

图2 等效东向/北向/天向随机游走引起的北向速度误差标准差理论和仿真比较

Fig. 2 Comparison of theory and simulation standard deviation of north velocity error due to equivalent east/north/up ARW

4 随机游走对系统性能的影响分析

根据前述得到的随机游走引起的导航误差的解析表达式(15),结合图1、图2、图3,可以看出:

(1) 观察公式(15),随机游走引起的每一项导航参数误差解析表达式中都包含有时间的平方根项,这表明随机游走引起的导航误差是以$\sqrt{t}$的方式无限增长的,从图中曲线的发散趋势也可以直观地看出这一规律,这与随机游走的误差特性相吻合;

(2) 随机游走导致的系统误差在不同的时间段增长速度不同,例如,东向随机游走激励下的北向速度误差在第1小时内增长很快,而在第6 - 10小时

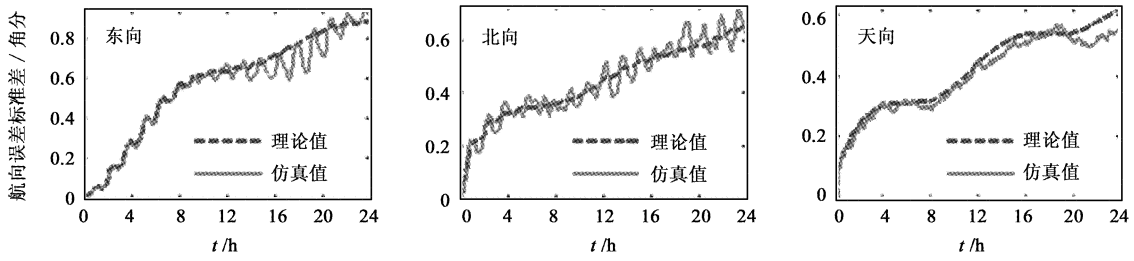

图 3　等效东向/北向/天向随机游走引起的航向误差标准差理论和仿真比较

Fig. 3　Comparison of theory and simulation standard deviation of heading error due to equivalent east/north/up ARW

内基本不变,因此,估计随机游走引起的系统误差时还应该考虑当前的工作时间;

(3) 不同方向上的随机游走对系统性能的影响程度不同,相比水平方向,天向陀螺随机游走对系统精度的影响较小。

5　结　论

由于随机游走误差不能通过一般的旋转调制、滤波等方法有效抑制,所以随机游走误差成为限制高精度光纤惯导系统最终精度的重要因素。根据随机游走的形成过程,可以将随机游走引起的导航误差视为系统在不相关的随机脉冲序列激励下的输出,从统计角度采用随机过程线性变换冲激响应法推导出随机游走引起的导航误差理论公式,从理论上揭示了随机游走误差在导航过程中的传播规律。根据推导出的理论公式可以在任意时间段内对每一只陀螺随机游走引起的导航误差进行定量估计。在此基础上,对比分析了三个正交方向上等效的陀螺随机游走对系统性能的影响。结果表明,天向陀螺随机游走引起的导航误差较小。由此可以根据具体的任务剖面对不同方向上的陀螺指标进行分配,这对于惯导系统的设计工作具有实际的工程指导意义。

参　考　文　献

[1] Barbour N, Schmidt G. Inertial sensor technology trends[J]. IEEE Sensor Journal,2001, 1(4): 332 - 339.

[2] Adams G, Gokhale M. Fiber optic gyro based precision navigation for submarines[C]. AIAA Guidance, Navigation, and Control Conference, Denver,USA,2000.

[3] 李家垒,许化龙,何婧. 光纤陀螺随机漂移的实时滤波方法研究[J]. 宇航学报,2010,31(12):2717 - 2721. [Li Jia-lei, Xu Hua-long, He Jing. Real-time filtering methods of random drift of fiber optic gyroscope[J]. Journal of Astronautics,2010,31(12): 2717 - 2721.]

[4] 刘建锋,江涌,丁传红. 基于 Kalman 光纤陀螺的随机信号处理[J]. 宇航学报,2009,30(2):604 - 608. [Liu Jian-feng, Jiang Yong, Ding Chuan-hong. Based on Kalman filter processing of FOG signal[J]. Journal of Astronautics, 2009,30(2):604 - 608.]

[5] 朱奎宝,张春熹,张小跃. 光纤陀螺随机漂移 ARMA 模型研究[J]. 宇航学报,2006,27(5):1118 - 1121. [Zhu Kui-bao, Zhang Chun-xi, Zhang Xiao-yue. Study on modeling and identification of random drift for FOG [J]. Journal of Astronautics,2006, 27(5):1118 - 1121.]

[6] 宋凝芳,张中刚,李立京,等. 光纤陀螺随机游走系数的分析研究[J]. 中国惯性技术学报,2004,12(4):34 - 38. [Song Ning-fang, Zhang Zhong-gang, Li Li-jing, et al. Random walk coefficient of fiber optic gyro[J]. Journal of Chinese Inertial Technology,2004,12(4):34 - 38.]

[7] 祝树生,任建新,张安峰. 光纤陀螺随机游走分析方法研究[J]. 应用光学,2009,30(6):1003 - 1006. [Zhu Shu-sheng, Ren Jian-xin, Zhang An-feng. Random walk analysis of fiber optic gyroscope[J]. Journal of Applied Optics,2009, 30(6):1003 - 1006.]

[8] 孙国飞,吴衍记,那永林. 光纤陀螺中随机游走的分析研究[J]. 战术导弹技术,2009(1):75 - 78. [Sun Guo-fei, Wu Yan-ji, Na Yong-lin. Investigation into random walk in optical fiber gyroscope[J]. Tactical Missile Technology,2009(1):75 - 78.]

[9] 王学勤,金靖,宋凝芳,等. 星载光纤陀螺的最优调制深度[J]. 宇航学报,2011,32(11):2346 - 2350. [Wang Xue-qin, Jin Jing, Song Ning-fang, et al. Optimum modulation depth in spacecraft-borne IFOG[J]. Journal of Astronautics, 2011,32(11):2346 - 2350.]

[10] 朱奎宝,张春熹,宋凝芳. 光纤陀螺角度随机游走对惯导系统影响[J]. 压电与声光,2007,29(3):292 - 294. [Zhu Kui-bao, Zhang Chun-xi, Song Ning-fang. Effection of angle random walk of fiber optic gyro (FOG) on INS [J]. Piezoeltectrics & Acoustooptics, 2007, 29(3):292 - 294.]

[11] 张仲毅,徐烨烽,李魁,等. 长航时惯导系统的随机游走误差传播规律及抑制方法[J]. 系统工程与电子技术,2011,33

(9): 2050 - 2054. [Zhang Zhong-yi, Xu Ye-feng, Li Kui, et al. Angle random walk error propagation and suppression methods in long-term inertial navigation system[J]. Systems Engineering and Electronics, 2011, 33(9): 2050 - 2054.]

[12] Levinson E. Laser-gyro strapdown inertial navigation system applications[R]. AGARD Lecture Series 95 on Strapdown Inertial Systems, London: Technical Editing and Reproduction Ltd Harford House, 1978.

[13] Kuritsky M M, Goldstein M S, Greenwood I A. Inertial Navgation-RLG Strapdown System Design Viewpoint[J]. Proceedings of the IEEE, 1983, 71(10): 1156 - 1170.

[14] Flynn D J. The effect of gyro random walk on the navigation performance of a strapdown inertial navigator[C]. Symposium on Gyro Technology, Stuttgart, Germany, 1982.

[15] Aboelmagd N D, Irvine-Halliday, Herb T, et al. New technique for reducing the angle random walk at the output of fiber optic gyroscopes during alignment processes of inertial navigation systemtems[J]. Optical Engineering, 2001, 40(10): 2097 - 2106.

[16] David H T, John L W. Strapdown inertial navigation technology[M]. 2nd Edition. United Kingdom & USA: the Institution of Engineering and Technology, and the American Institute of Aeronautics and Astronautics, 2004.

[17] Savage P G. Strapdown analytics[M]. Minnesota: Strapdown Associates, Inc., 2000.

[18] Britting K R. Inertial navigation systems analysis[M]. New York: Wiley Interscience, 1971.

[19] 周荫清. 随机过程理论[M]. 第2版. 北京: 电子工业出版社, 2006: 105 - 107.

作者简介:

任磊(1982 -),男,博士生,研究方向为导航、制导与控制技术。

通信地址:北京市142信箱402分箱 重点室(100854)

电话:(010)68763592

E-mail:rlli2001@163.com

(编辑:曹亚君)